

EXPERIMENTAL STUDIES OF SEISMOELECTRIC MEASUREMENTS IN A BOREHOLE

Zhenya Zhu, Matthijs W. Haartsen, and M. Nafi Toksöz

Earth Resources Laboratory
Department of Earth, Atmospheric, and Planetary Sciences
Massachusetts Institute of Technology
Cambridge, MA 02139

ABSTRACT

Experimental and theoretical studies show that there are two kinds of electromagnetic (EM) fields generated by seismic waves in a fluid-saturated porous medium. First, at an interface where the formation properties are different, the generated seismoelectric wave is a propagating electromagnetic wave that can be received anywhere. The second kind of field occurs inside a homogeneous formation where the seismic wave generates an electromagnetic field which exists only in the area disturbed by the seismic wave and whose apparent velocity is that of the seismic wave. An electrode, used as a receiver located on the ground surface, can only receive the propagating EM wave. However, when an electrode is in a borehole and close to the porous formation, it can receive both of the above EM waves. In this study, electrokinetic measurements are performed with borehole models made of natural rocks or artificial materials. The results of the experiment show that the Stoneley wave and other acoustic modes excited by a monopole source in the borehole models generate seismoelectric waves in fluid-saturated formations. The electrical components of the seismoelectric waves can be received by an electrode in the borehole or on the borehole wall. The amplitude and frequency of the seismoelectric wave are related not only to the seismic wave, but also to the formation properties, such as permeability, conductivity, etc. Therefore, seismoelectric logging may explore different properties of the formation than those investigated by standard acoustic logging. Electrostatic measurements are also performed with these borehole models. The electric pulse introduced through the electrode in the borehole or on the borehole wall induces a Stoneley wave in the fluid-saturated model which can be received by a monopole transducer in the same borehole. These measurement methods, seismoelectric logging or electrostatic logging, can be applied to field borehole logging to investigate formation properties relating to pore fluid flow.

INTRODUCTION

Because of the electro-chemical effects on the interfaces between solid and fluid in a fluid-filled porous medium, there is a phenomenon known as the electric double layer on the solid surface and free charges in the pore fluid (Bellugi, 1937; Martner and Sparks, 1959; Broz and Epstein, 1976; Neev and Yeatts, 1989; Haartsen, 1995; Haartsen and Toksöz, 1996). When a seismic wave propagates in the medium, the charge motion generates an electromagnetic field. This is the seismoelectric conversion (Chandler, 1981; Ishido and Mizutani, 1981; Morgan *et al.*, 1989; Zhu *et al.*, 1994; Jouniaux and Pozzi, 1995). On the other hand, when an electric field induces a relative motion of the free charges in the pore fluid against a solid matrix, the interaction between the pore fluid and the solid generates an electroseismic wave. This is the electroseismic conversion (Kozak and Davis, 1989; Pride and Haartsen, 1996; Zhu *et al.*, 1997).

The generated seismoelectric signals relate not only to the seismic waves, but also to the conductivity (or resistivity) of the pore fluid and the permeability of the formation (Cerdeña and Kiry, 1989; Kuin and Stein, 1987; Pride, 1994). When the properties of the contacting formations, such as conductivity, permeability, rock grains, etc., are different from each other, a physical interface is formed between the two formations. Because of the imbalance of the free charges in the pore fluid at the interface, the seismic wave generates a free electromagnetic wave propagating at light speed, which is much faster than that of any acoustic wave. Inside the homogeneous medium, the charges are balanced in the areas disturbed by the seismic wave, which generates a seismoelectric field in the disturbed area, but does not generate a seismoelectric wave outside the area. This seismoelectric wave is a local EM wave and does not propagate in the medium. Its apparent velocity is the same as the seismic velocity (Pride and Haartsen, 1996; Zhu and Toksöz, 1996; Zhu *et al.*, 1996).

Many previous measurements were conducted on the earth's surface or in shallow boreholes (Thompson and Gist, 1993; Butler *et al.*, 1994; Mikhailov *et al.*, 1997). Only seismoelectric signals generated at an interface can be received. It is difficult to apply this measurement to explore deep formations due to the low efficiency of the seismoelectric conversion and the high attenuation in the formations.

In this paper, we investigate a logging method that can measure both the propagating and the local seismoelectric waves by setting the electric receiver in a borehole. Since the electrode is close to the borehole formation, stronger signals can be received with high measurement accuracy. If both the seismic source and the electrode are in a borehole, this method can explore deep formations and can be applied to petroleum geophysics.

In our study, several ultrasonic borehole models are made of natural rocks and artificial materials. We measured the seismoelectric signals with different logging methods, investigated the seismoelectric fields at different formations, and compared them with the acoustic waves in the boreholes. We also measured and compared the electroseismic waves generated by an electric pulse with high voltage at the different sections of the

Laboratory Seismoelectric Measurements

borehole models.

BOREHOLE MODELS AND MEASUREMENT SYSTEM

The simplest borehole model is a sandstone cylinder with a borehole of 1.27 cm in diameter along its axis. Other models are made of two different materials to simulate different formations and an interface (Figure 1). The sizes and materials of the five borehole models we used are listed in Table 1. The glued sand with large permeability is made of fine quartz sand glued with epoxy. Some electrodes are buried on the borehole wall inside the glued sand. The properties of the materials are listed in Table 2.

For the measurements of the seismoelectric conversion, a PZT transducer 0.9 cm in diameter, is the seismic source which is excited by an electric square pulse of 0.01 ms in width and 750 V in amplitude. The electrode is a point receiver, 0.05 cm in diameter and 0.1 cm in length, made of a shielding cable wire. The received seismoelectric signals are displayed and recorded on a digital oscilloscope after going through an amplifier and a filter (Zhu *et al.*, 1996). The borehole models are put in a vacuum system and saturated with water, and then the models and the source transducer, as well as the point electrode, are put in a water tank. To compare the seismoelectric field with the acoustic field in the boreholes, the experiments are repeated with a hydrophone (B & K 8103) replacing the electrode to measure the acoustic fields.

For the measurements of the electroseismic conversion, an electrode emitting a high-voltage pulse is the source. A hydrophone is used to receive and record the electroseismic waves.

All received waveforms are recorded with a certain time delay to avoid the huge electric influence of the high voltage pulse. The amplitudes of the waveforms are normalized by the maximum amplitude in each plot. The maximum amplitude of the seismoelectric signals in our experiments is around 0.1 mV.

SEISMOELECTRIC CONVERSION

The goal of the experiments described in this section is to confirm that seismic waves in a borehole, particularly the Stoneley wave, generate seismoelectric signals. Later we will investigate the seismoelectric field in a borehole. In the other words, first we fix the electrode and move the seismic source in the boreholes (Figure 2). Then we investigate the seismoelectric field in a borehole. We will move the electrode to measure the seismoelectric signals in the boreholes when the seismic source is fixed. To compare this with the acoustic field in the borehole, we replace the electrode with a hydrophone to record the acoustic waves under the same conditions.

Figure 3 shows the acoustic waves (Figure 3a) and the seismoelectric waves (Figure 3b) in the sandstone model (Model 1), when the electrode is fixed in the borehole center and the acoustic source is moved along the borehole axis. Because of the excitation and the attenuation in the sandstone borehole, the frequency of the Stoneley wave is very

low (about 20 kHz), but the frequency of the P-wave and pseudo-Rayleigh wave are much higher (about 150 kHz). From the slope of the seismoelectric signals in Figure 3b, we know that the Stoneley wave and the low-frequency component of the P-wave generate the seismoelectric waves.

Figure 4 shows the acoustic waves (Figure 4a) and the seismoelectric signals (Figure 4b) in Model 2. Because the seismic source is located in the Lucite section, only P-wave and Stoneley waves can be excited in the borehole. We can observe the corresponding seismoelectric signals from the electric waveforms (Figure 4b) received by the electrode fixed in the sandstone section.

In Model 3, shown in Figure 2, a set of point electrodes made of wires is buried in the borehole wall. Both the electrodes in the borehole and on the wall receive the seismoelectric signals. When the acoustic source moves in the Lucite section of the borehole, the received signals are as shown in Figure 5a and 5b, respectively.

The above experiments confirm that seismic waves in a borehole generate seismoelectric signals in the borehole formation which can be received by an electrode in the borehole center or the borehole wall. The results show that the seismoelectric signals are generated in the wall formation and their apparent velocities are the same as those of the seismic waves. Therefore, they are local, nonpropagating seismoelectric waves.

We replace the monopole transducer in the borehole of Model 3 with a plane transducer located on the upper side of the Lucite cylinder (Figure 2). Figure 6 show the seismoelectric signals received by electrodes #1, #2, #3, and #4 buried in the borehole wall. From the recorded waveforms, we see that the arrival times of the first maximum wave vary with the depth of the electrodes. Therefore the first maximum arrivals are the local seismoelectric signals generated by the seismic wave which arrives at the electrode. We can also see waves with small amplitude before the first maximum arrivals in the waveforms received by electrode #3, and #4 (Figure 6). Their arrival times are the same as the first arrivals of the seismoelectric wave on the electrode #1. Thus, we conclude that the small wavelets are the seismoelectric signals generated at the interface between the Lucite and the glued sand. They propagate in the medium with the electromagnetic wave velocity and decay according to the attenuation of the electromagnetic wave.

SEISMOELECTRIC FIELD

The following experiments show the whole seismoelectric field generated by the seismic source in a borehole (Figure 7). The seismoelectric waves are recorded in Figure 8 when a source is fixed in material 1 and the electrode moves from material 2 across the interface to material 1. The measurements are conducted using Models 3, 4 and 5; both the seismic field and seismoelectric field are shown in Figure 8. The electrode (or the hydrophone) for the fifth trace in the plots is located at the interface.

The seismic waves in material 1 are the strongest and decrease with the distance from the source. If the impedances of the two materials are close to each other (such as

Laboratory Seismoelectric Measurements

in Model 3), the seismic waves have no obvious change when passing from one to the other (Figure 8a).

The strength of the seismoelectric field depends not only on the strength of the seismic waves, but also on the properties of the material. In materials with low porosity and permeability, such as Lucite and slate, only very weak seismoelectric signals are generated, even though the seismic waves are strong. In the opposite case, in porous materials such as sandstone and glued sand, the generated seismoelectric signals are much stronger. Note that the seismoelectric signals with high frequency are generated at the interface, and received by the near electrodes (Figures 8b, 8d, and 8f). Comparing the waveforms of the 4th, 5th, and 6th traces in Figures 8b, 8d, and 8f, we know that the first arrival times are the same due to the high velocity in the borehole. This means that seismic waves generate the propagating seismoelectric waves at the interface between the materials and generate the local, nonpropagating seismoelectric signals inside the porous materials.

Comparing the seismoelectric waves with seismic waves, we know that they are based on a different mechanism and relate to different properties of the wall formation. Therefore, seismoelectric logging could be a new logging method to explore the physical properties related to fluid flow in the wall formation.

ELECTROSEISMIC CONVERSION

The above experiments have examined the seismoelectric signals generated by seismic waves in a borehole. In this section, we investigate the electroseismic conversion in a borehole. In this case we receive the seismic waves induced by an electric signal. The source is the electrode emitting a high-voltage electric pulse and the receiver is a seismic transducer in the borehole. We investigate the electroseismic waves induced by the electrode in the borehole or on the borehole wall, and the variation of the electroseismic waves when the electrode is moved along the borehole (Figure 9). Figure 10 shows the electroseismic waves received by an acoustic transducer moving in the Lucite section with an increase of 1 cm/trace when the positive pole of the electrode is located in the glued sand section. The amplitude of the square pulse coming from the electrode is about 500 V. When the width of the square pulse is matched to the half period of the received seismic wave, the amplitude of the seismic wave is at maximum. From the moveout of the received electroseismic waves, we calculate the phase velocity (1050m/s) and know that they are Stoneley waves in the borehole.

When the electrodes are on the borehole wall (electrodes 2-2 in Figure 9), the electric pulse also generates a Stoneley wave (Figure 11). The waveforms in Figure 10 and Figure 11 are slightly different, but they propagate with the same velocity.

In the above experiments we fixed the electrodes and moved the acoustic receiver. If we fix the acoustic receiver and move the electrode, a new set of seismic waves can be recorded (Figure 12). From the seismic diagram we know that the electric pulse generates electroseismic waves in the porous formation section that propagate with the

Stoneley wave velocity along the borehole. The closer the electrode is to the acoustic receiver, the stronger the amplitude of the electroseismic waves and the earlier the arrival times. If the electrode is located at the Lucite section without permeability, no seismic wave can be generated. The results show that the electric pulse can generate the electroseismic wave through the electrode near the porous borehole wall and the wave propagates in the borehole with Stoneley wave velocity due to its low frequency.

CONCLUSIONS

We studied both seismoelectric and electroseismic conversions experimentally with various borehole models. The seismic waves generate seismoelectric signals and the electric pulses induce electroseismic waves in a fluid-saturated porous borehole due to the conversions. The results of this experiment show that the seismoelectric signals or the electroseismic waves can be generated only in the sections of the sandstone or the artificial porous materials where the source and the receiver are in the same fluid-filled borehole. In the borehole sections surrounded by a homogeneous porous formation, the generated seismoelectric signal is a stationary, local electromagnetic wave whose apparent velocity is the seismic wave velocity. At the interface between the formations with different physical properties, the seismic wave in the borehole generates a seismoelectric signal propagating with light speed in the borehole. The seismoelectric field is different from the acoustic field in the borehole due to the mechanism of the seismoelectric conversion. The seismoelectric signals depend on the pore fluid properties such as conductivity, porosity, permeability, etc. The experimental results confirm the possibility of a new borehole logging technique in a fluid-filled borehole to explore more physical properties related to the fluid and its flow in the porous formations. In this paper we do not investigate the frequency response of the seismoelectric conversion in a borehole in detail. More experiments are needed in the future.

ACKNOWLEDGMENTS

We thank Dr. A. H. Thompson, Prof. S. R. Pride, and Prof. T. R. Madden for their valuable suggestions and useful discussions. This work was supported by the Borehole Acoustics and Logging Consortium at the Massachusetts Institute of Technology and by the Department of Energy grant DE-FG02-93ER14322.

Laboratory Seismoelectric Measurements

REFERENCES

- Belluigi, A., 1937, Seismic-electric prospecting; *The Oil Weekly*, 38-42.
- Butler, K., R. Russell, A. Kepic and M. Maxwell, 1994, Mapping of a stratigraphic boundary by its seismoelectric response, *Proceedings on the Applications of Geophysics to Engineering and Environmental Problems (SAGEEP)*, 689-699.
- Butler, K., R. Russell, A. Kepic and M. Maxwell, 1996, Measurement of the seismoelectric response from a shallow boundary, *Geophysics*, 61, 1769-1778.
- Broz, Z., and N. Epstein, 1976, Electrokinetic flow through porous media composed of fine cylindrical capillaries, *J. of Colloid and Interface Science*, 56, 605-612.
- Cerda, C.M., and Non-Chhom Kiry, 1989, The use of sinusoidal streaming flow measurements to determine the electrokinetic properties of porous media, *Colloids and Surfaces*, 35, 7-15.
- Chandler, R., 1981, Transient streaming potential measurements on fluid saturated porous structures: An experimental verification of Biot's slow wave in the quasi-static limit, *J. Acoust. Soc. Am.*, 70, 116-121.
- Haartsen, M.W., 1995, Coupled electromagnetic and acoustic wavefield modeling in poro-elastic media and its applications in geophysical exploration, Ph.D. thesis, M.I.T.
- Haartsen, M.W., and M.N. Toksöz, 1996, Dynamic streaming currents from seismic point sources using relative flow green's functions in isotropic poro-elastic media (submitted), *Geophys. J. Internat.*
- Haartsen, M.W., Z.Zhu, and M.N. Toksöz, 1995, Seismoelectric experimental data and modeling in porous layer models at ultrasonic frequencies, SEG 65th Annual International Meeting Expanded Abstracts, PP5.10, 696-699, Houston.
- Ishido, T. and H. Mizutani, 1981, Experimental and theoretical basis of electrokinetic phenomena in rock-water system and its applications to geophysics, *J. Geophys. Res.*, 86, 1763-1775.
- Journiaux, J., and J. Pozzi, 1995, Streaming potential and permeability of saturated sandstones under triaxial stress: Consequences for electrotelluric anomalies prior to earthquakes, *J. Geophys. Res.*, 100, 10197-10209.
- Kozak, M.W., and E.J. Davis, 1989, Electrokinetics of concentrated suspensions and porous media, *J. Colloid and Interface Science*, 127, 497-510 and *J. Colloid and Interface Science*, 129, 166-174.
- Kuin, A.J., and H.N. Stein, 1987, Development of a new pore model: II Electrokinetic transport properties, surface conductance, and convective charge transport, *J. Colloid and Interface Science*, 115, 188-198.
- Martner, S.T., and N.R.Sparks, 1959, The electroseismic effect, *Geophysics*, 24, 297-308.
- Mikhailov O., M.W. Haartsen and M.N Toksöz, 1997, Electroseismic investigation of the shallow subsurface: field measurements and numerical modeling, *Geophysics*, 62, 97-105.

Zhu et al.

- Morgan, F.D., E.R. Williams, and T.R. Madden, 1989, Streaming potential properties of westerly granite with applications; *J. Geophys. Res.*, 94, No.B9, 12.449-12.461.
- Neev, J., and F.R. Yeatts, 1989, Electrokinetic effects in fluid-saturated poroelastic media, *Physical Review B*, 40, 9135-9142.
- Pride, S.R., 1994, Governing equations for the coupled electromagnetics and acoustics of porous media, *Physical Review B*, 50, 15678-15696.
- Pride, S.R. and M.W. Haartsen, 1996, Electroseismic wave properties (accepted), *J. Acoust. Soc. Am.*
- Thompson, A.H., and G.A. Gist, 1993 Geophysical applications of electrokinetic conversion, *The Leading Edge*, 12, 1169-1173.
- Zhu, Z., C.H. Cheng, and M.N. Toksöz, 1994, Electrokinetic conversion in a fluid-saturated porous rock sample, SEG 64th Annual International Meeting Expanded Abstracts, Paper SL1.1, 425-427.
- Zhu, Z., M.W. Haartsen, and M.N. Toksöz, 1996, Experimental studies of seismoelectric conversion in fluid-saturated porous media, Submitted to *Geophysics*.
- Zhenya Zhu and M.N. Toksöz, 1996, Experimental studies of seismoelectric conversion in fluid-saturated porous medium, SEG 66th Annual International Meeting Expanded Abstracts, RP1.6, 1699-1702, Denver, Colorado.
- Zhu, Z., M. W. Haartsen, and M.N. Toksöz, 1997, Experimental studies of electroseismic conversion in a fluid-saturated porous medium, this report, 12-1-12-18.

Laboratory Seismoelectric Measurements

Table 1: Configurations of the borehole models

Models	Model 1	Model 2	Model 3	Model 4	Model 5
Material 1	sandstone	Lucite	Lucite	slate	slate
Material 2	sandstone	sandstone	glued sand	sandstone	glued sand
D (cm)	1.27	1.5	1.27	1.27	1.27
L1 (cm)	12	6.5	14	20	20
L2 (cm)	12	7.5	5.5	9.0	5.5

Table 2: Physical parameters of the water-saturated samples

Sample	Density (g/cm^3)	Porosity (%)	Vp (m/s)	Vs (m/s)	Permeability (Darcy)
Sandstone	2.08	18.9	2900	1480	0.3
Glued Sand	1.71	25.6	2540	1200	190
Slate	2.65	0.5	4750	2650	0
Lucite	1.18	0.0	2700	1290	0

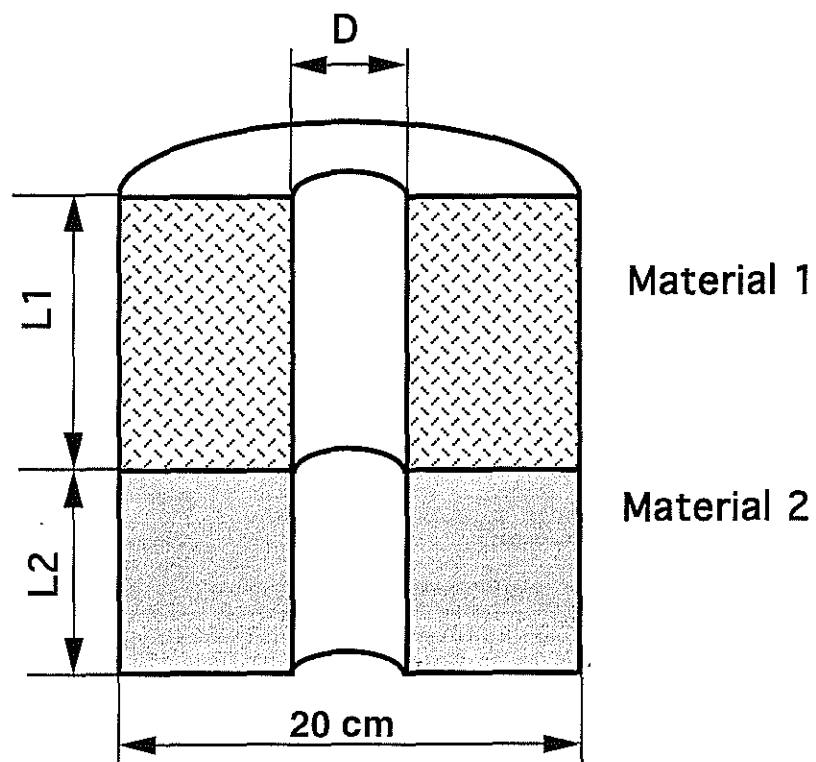


Figure 1: Diagram of ultrasonic borehole model. The sizes and materials are listed in Table 1. The properties of materials are listed in Table 2.

Laboratory Seismoelectric Measurements

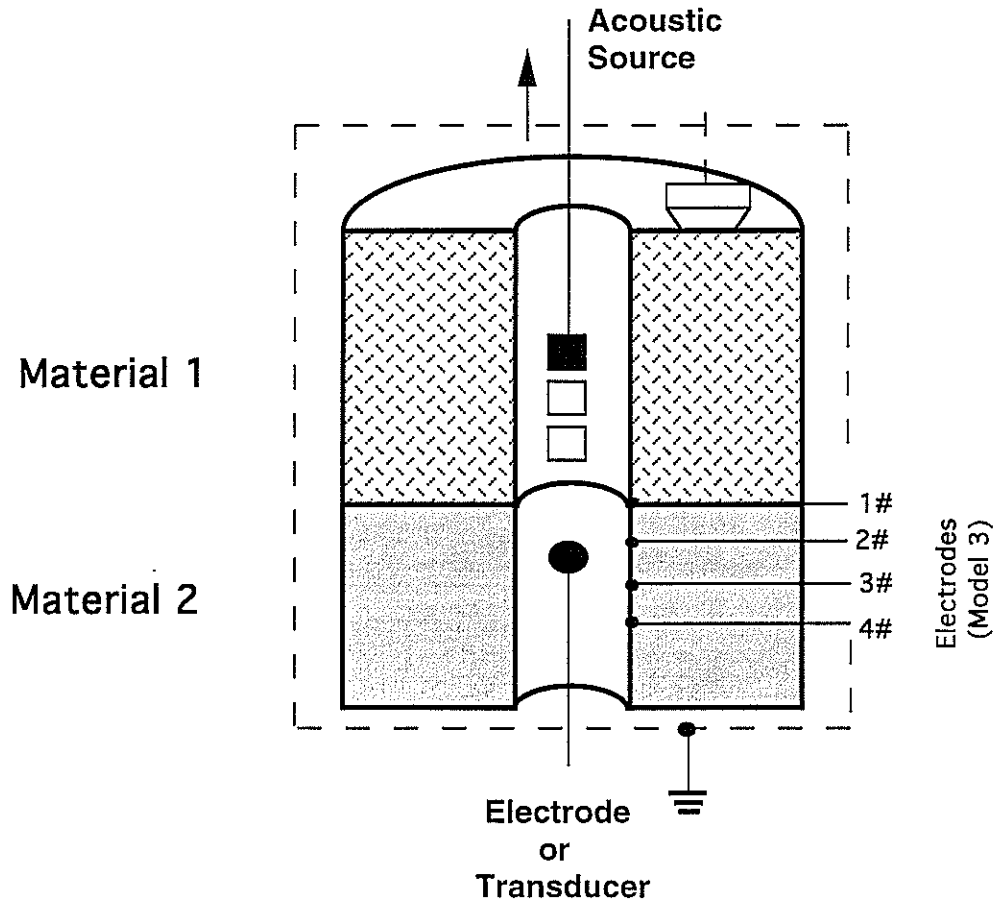


Figure 2: Diagram for measuring seismoelectric conversion in borehole models. The electric receiver is fixed in the section of Material 2 and the acoustic source is moved along the borehole or a plane transducer is fixed on the top side.

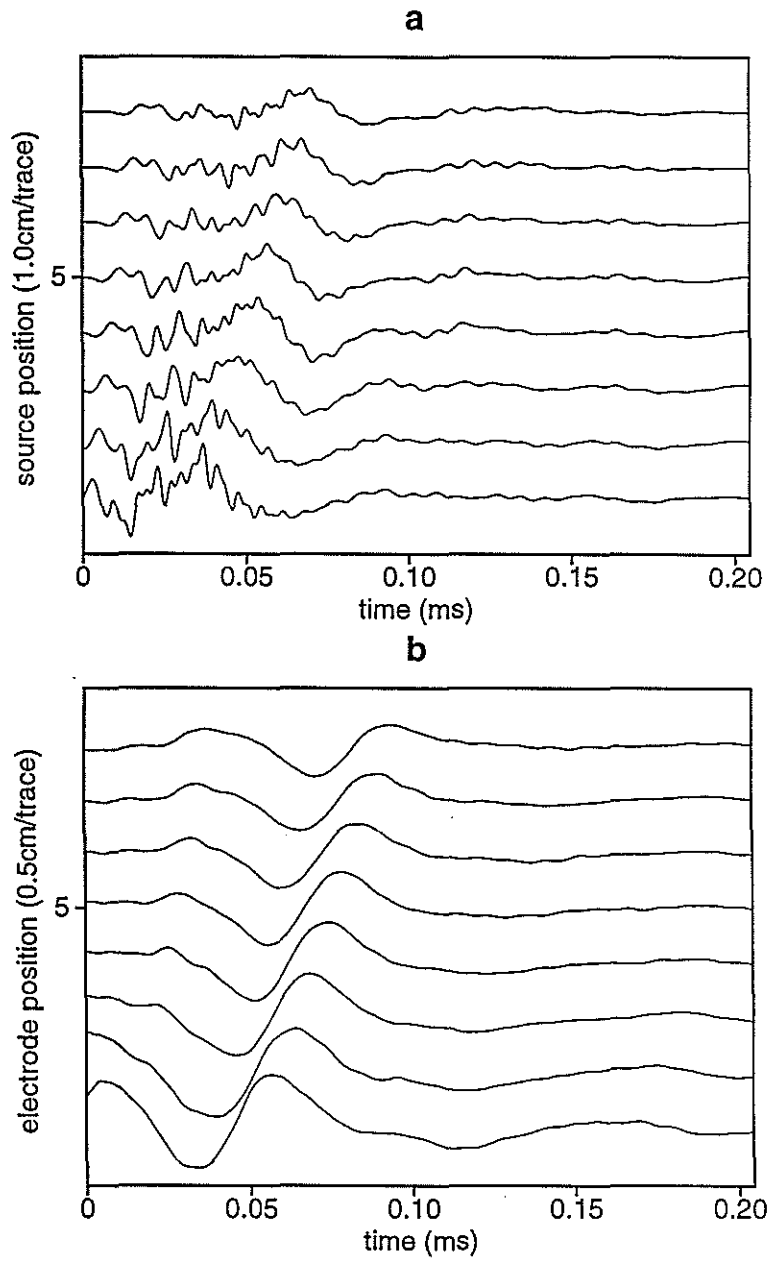


Figure 3: Acoustic waveforms (a) and the seismoelectric signals (b) in the sandstone borehole model (Model 1) recorded by fixing the acoustic or electric receiver and moving the acoustic source along the borehole.

Laboratory Seismoelectric Measurements

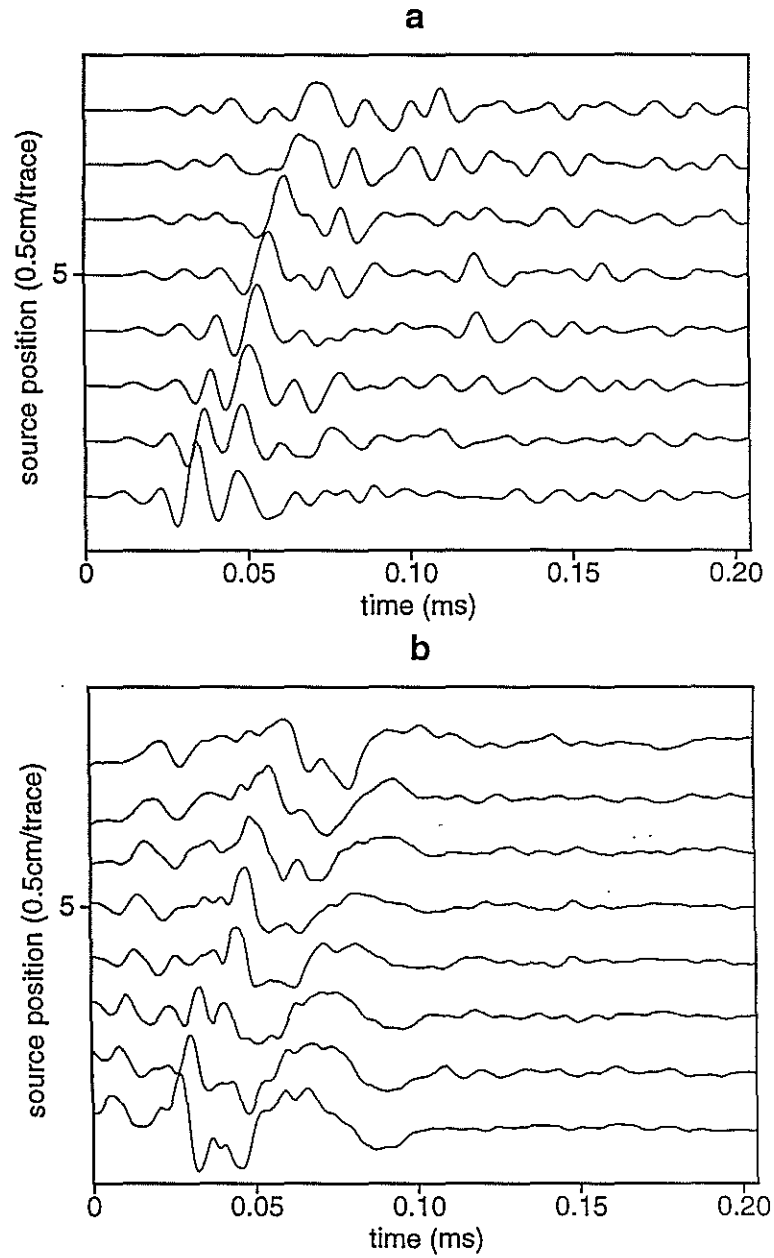


Figure 4: Acoustic waveforms (a) and electric signals (b) in Model 2 recorded by fixing the acoustic or the electric receiver in the sandstone section and moving the acoustic source in the Lucite section.

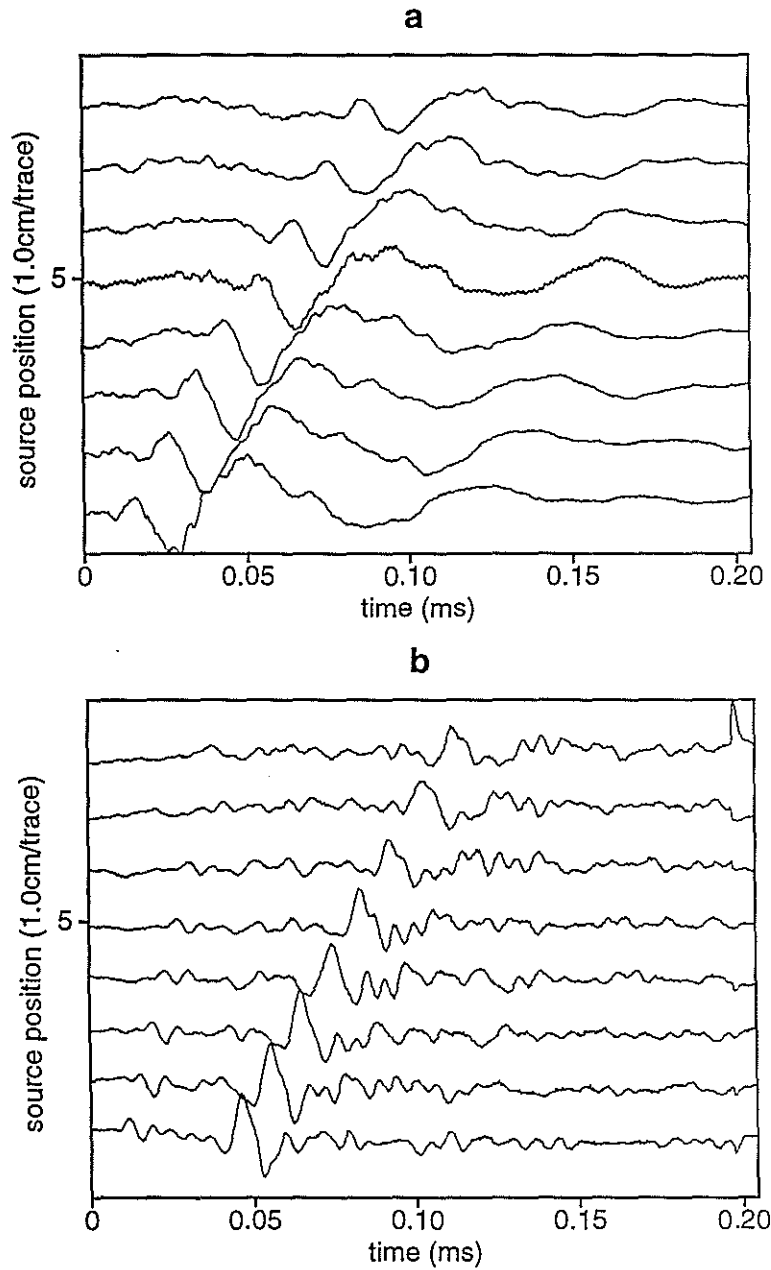


Figure 5: Seismoelectric signals received by the electrode in the borehole (a) or by the electrodes in the borehole wall (b) when the acoustic source moves in the Lucite section of Model 3.

Laboratory Seismoelectric Measurements

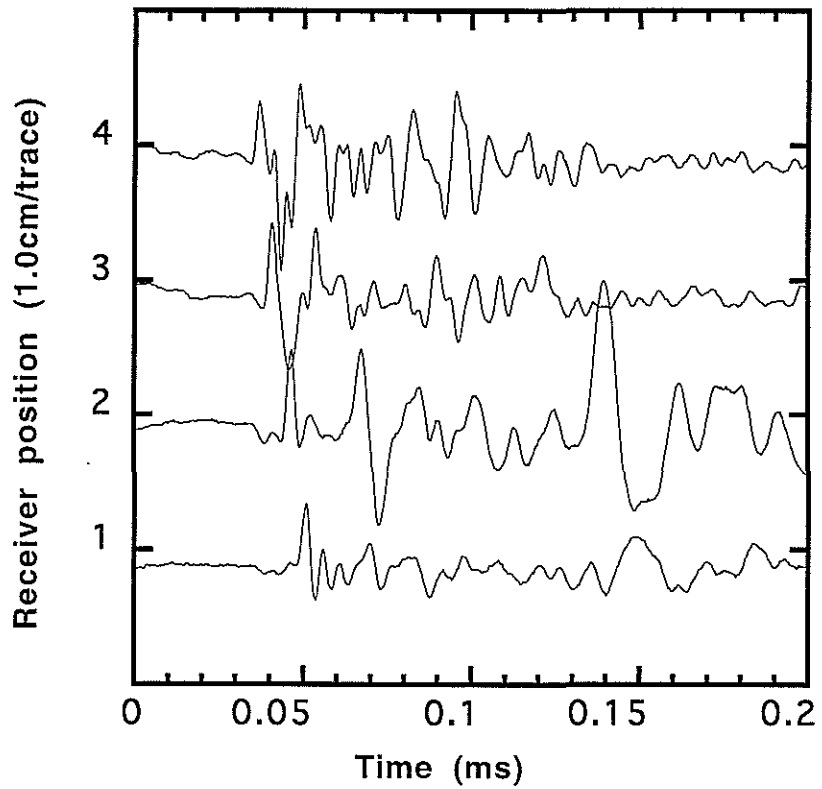


Figure 6: Seismoelectric signals received by the wall electrodes #1, #2, #3, and #4 of Model 3 when a plane acoustic source is fixed on the top side of Model 3.

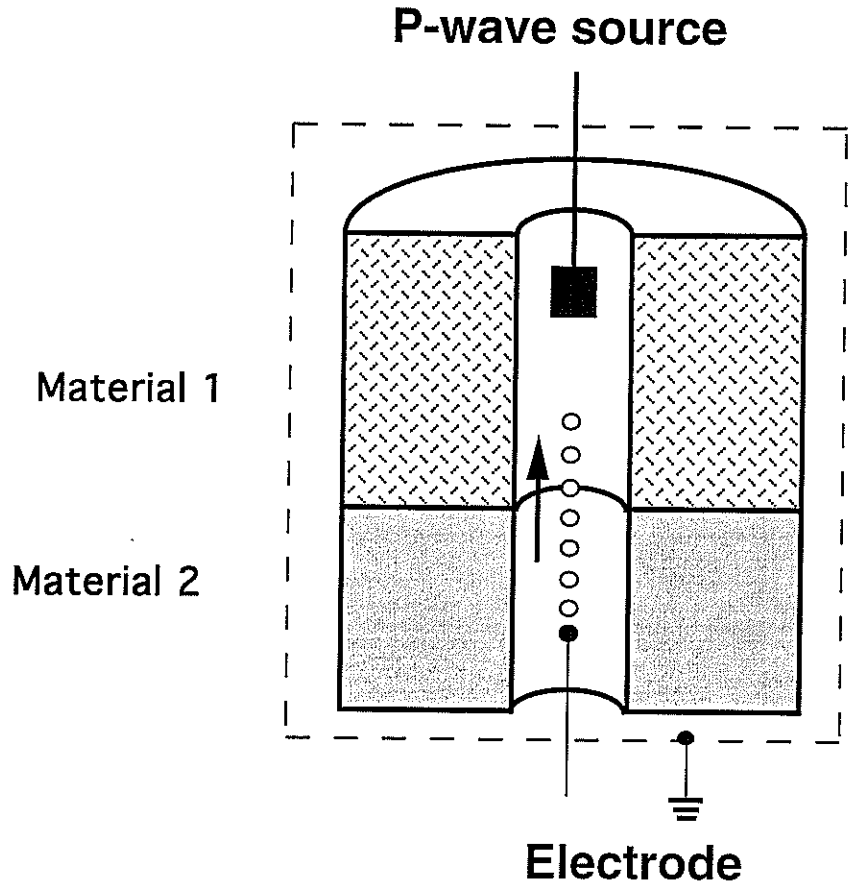


Figure 7: Diagram for measuring seismoelectric field in the borehole models with fixing the acoustic source and moving the electrode along the borehole.

Laboratory Seismoelectric Measurements

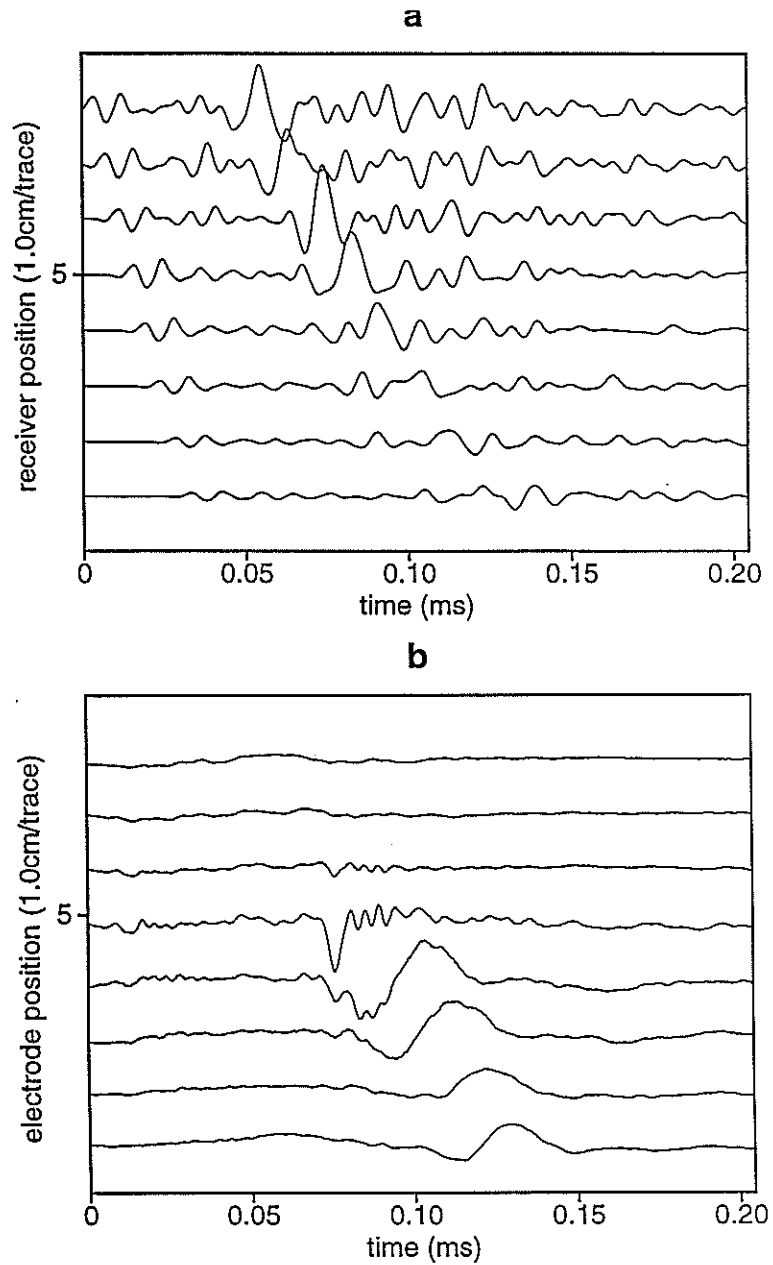


Figure 8: Acoustic waveforms (a) and seismoelectric signals (b) recorded in Model 3 when the acoustic source is fixed in the section of material 1 and the acoustic receiver or electrode moves from the section of material 2 to material 1. The fifth trace is located at the interface.

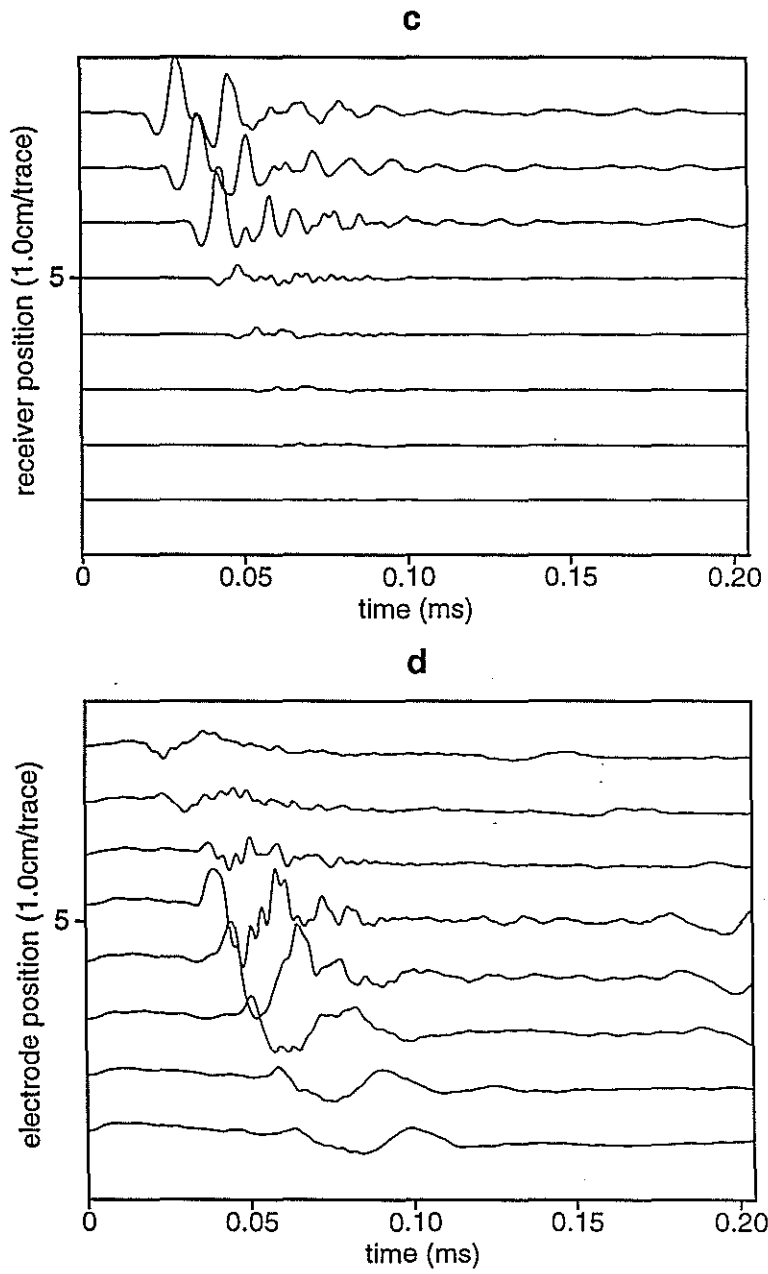


Figure 8, continued: Acoustic waveforms (c) and seismoelectric signals (d) recorded in Model 4 when the acoustic source is fixed in the section of material 1 and the acoustic receiver or electrode moves from the section of material 2 to material 1. The fifth trace is located at the interface.

Laboratory Seismoelectric Measurements

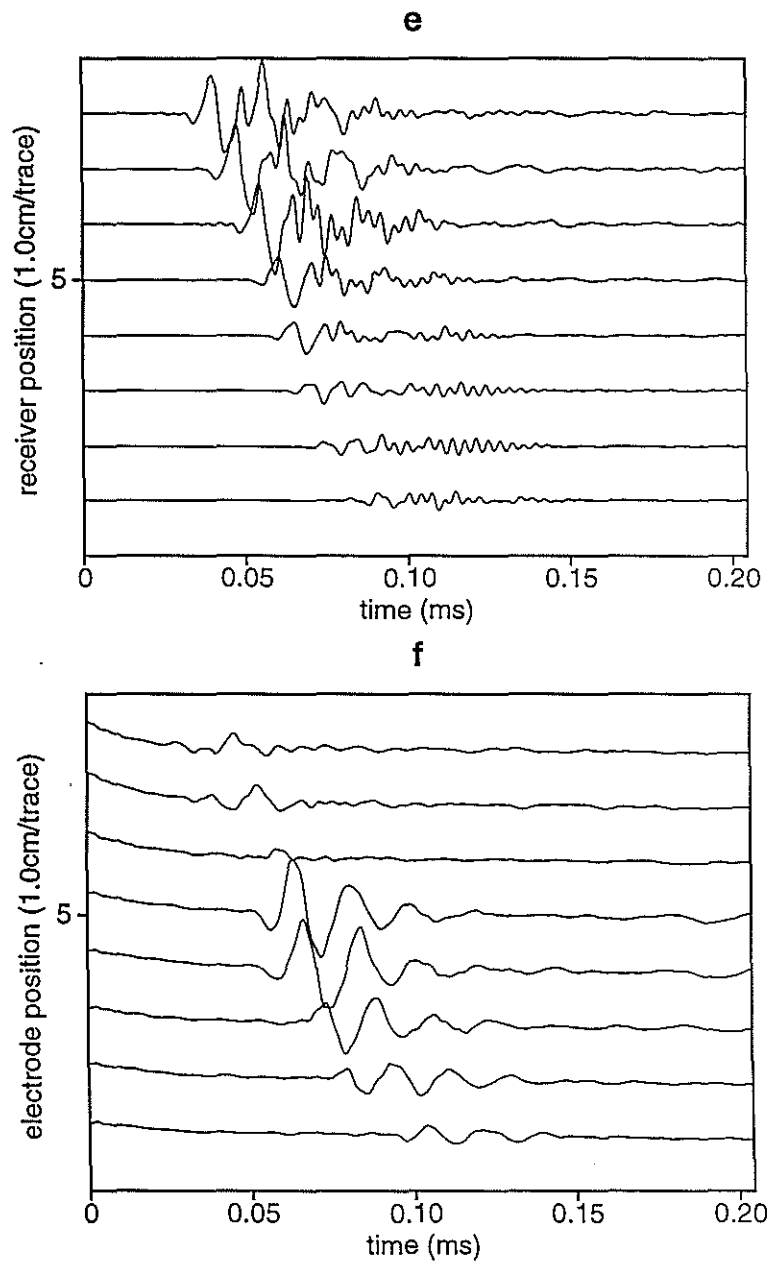


Figure 8, continued: Acoustic waveforms (e) and seismoelectric signals (f) recorded in Model 5 when the acoustic source is fixed in the section of material 1 and the acoustic receiver or electrode moves from the section of material 2 to material 1. The fifth trace is located at the interface.

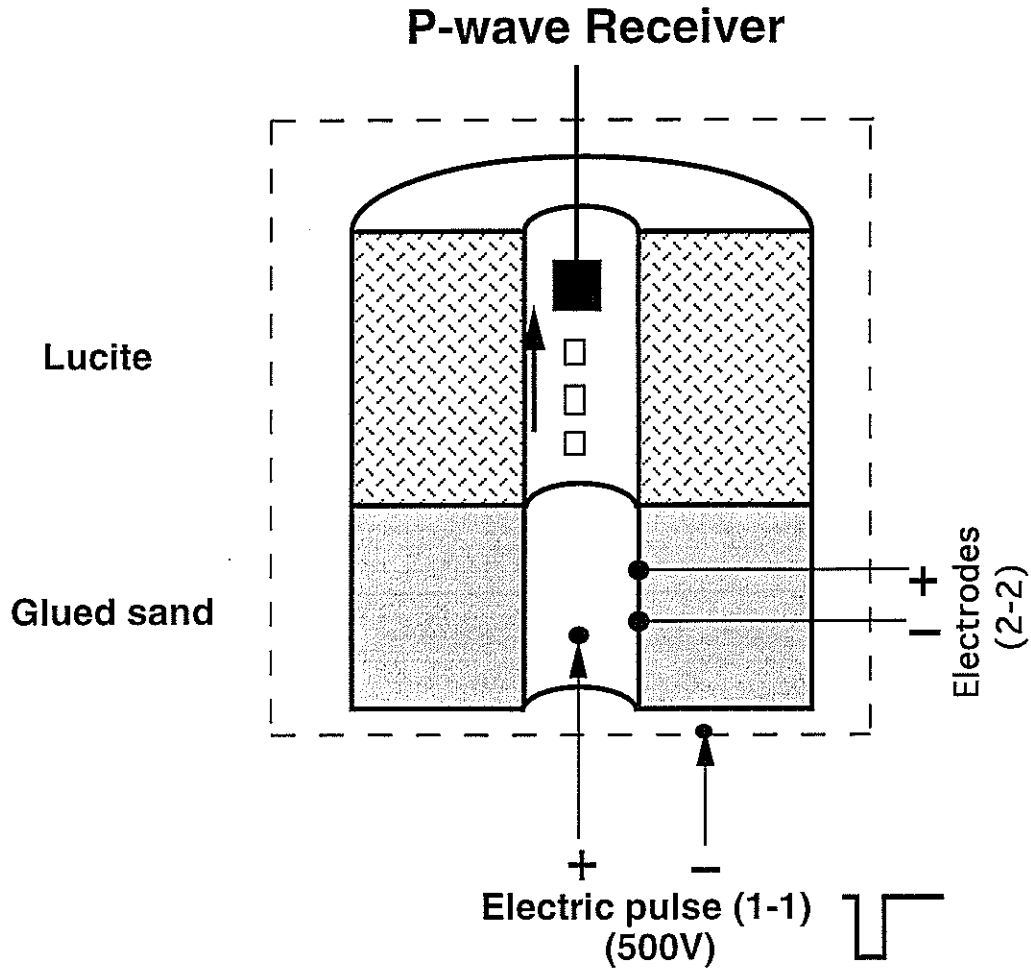


Figure 9: Diagram for measuring the electroseismic conversion in Model 3. The source electrodes are in the borehole (1-1) or in the borehole wall (2-2) and the acoustic receiver moves along the borehole.

Laboratory Seismoelectric Measurements

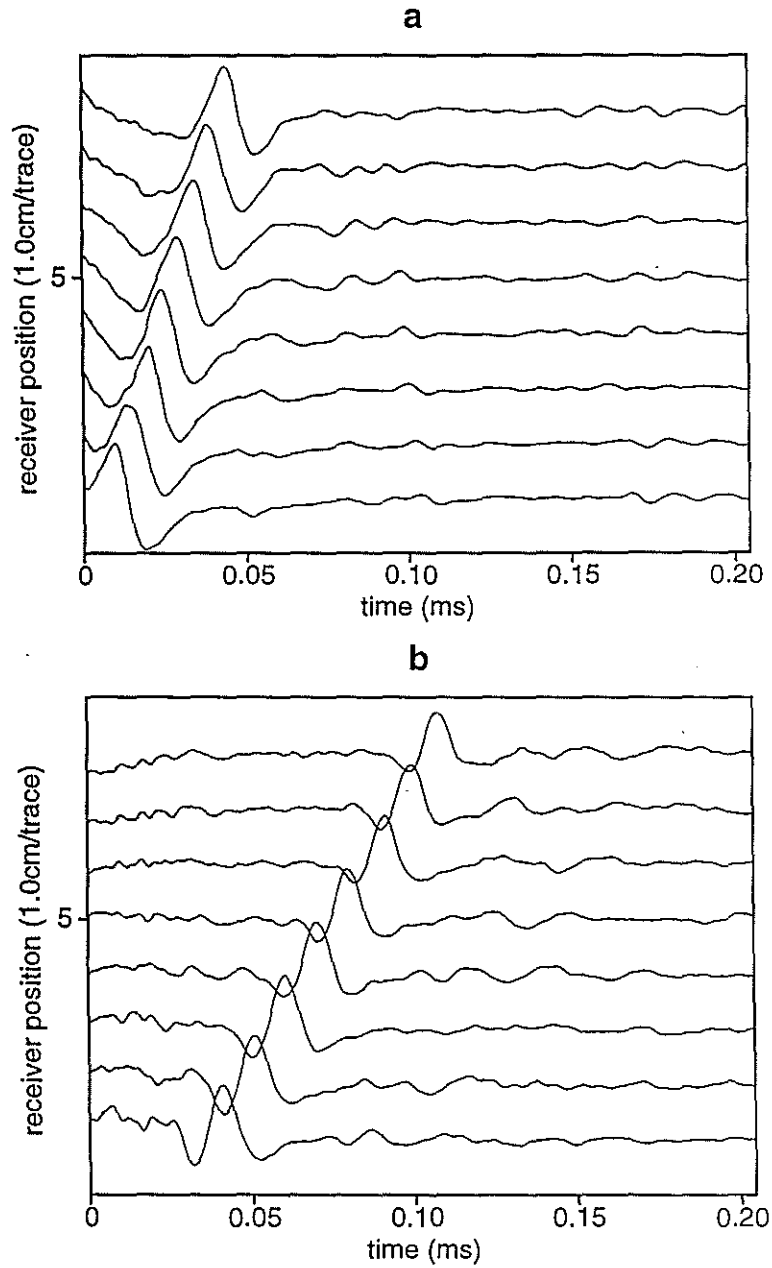


Figure 10: Electro seismic waveforms generated by the electrodes in the borehole (a) and the electrodes in the borehole wall (b) of Model 3 when the acoustic receiver moves in the Lucite section of the borehole.

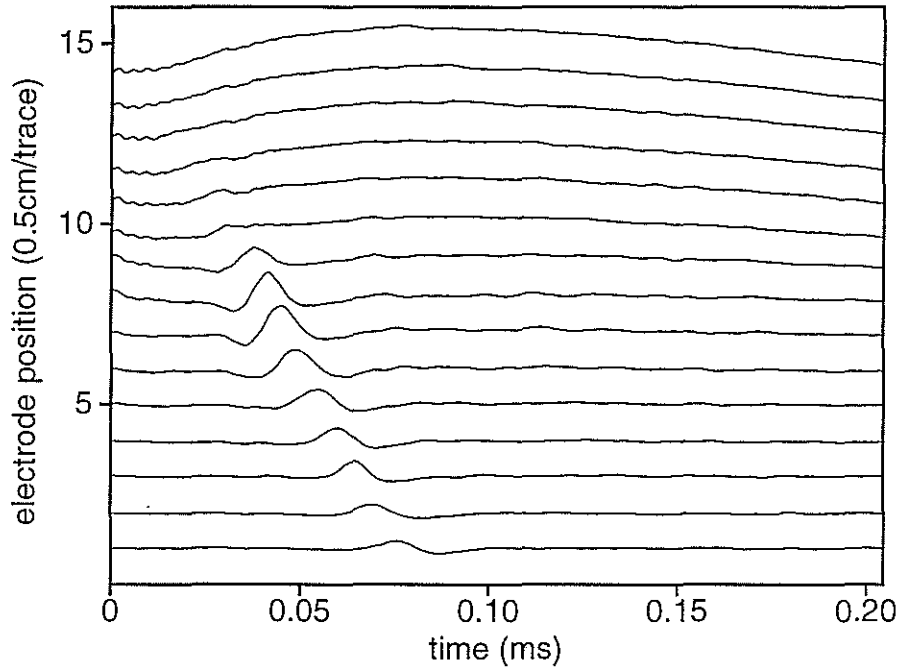


Figure 11: Electro seismic waveforms generated by an electrode moving from the glued-sand section to the Lucite section of Model 3 when the acoustic receiver is fixed in the Lucite section. The eighth trace is located at the interface.